DOI: 10.1021/ic901279t

Inorganic Chemistry
Article

# Design and Synthesis of a Fluorescent Probe for $Zn^{2+}$, 5,7-Bis(*N*,*N*-dimethylaminosulfonyl)-8-hydroxyquinoline-Pendant 1,4,7,10-Tetraazacyclododecane and $Zn^{2+}$-Dependent Hydrolytic and $Zn^{2+}$-Independent Photochemical Reactivation of Its Benzenesulfonyl-Caged Derivative

**Ryosuke Ohshima,[†] Masanori Kitamura,[†,‡] Akinori Morita,[§] Motoo Shiro,[∥] Yasuyuki Yamada,[†] Masahiko Ikekita,[§] Eiichi Kimura,[⊥] and Shin Aoki*[,†,‡]**

[†]*Faculty of Pharmaceutical Sciences, Tokyo University of Science, 2641 Yamazaki, Noda 278-8510, Japan,* [‡]*Center for Technologies against Cancer, Tokyo University of Science, 2641 Yamazaki, Noda 278-8510, Japan,* [§]*Faculty of Science and Technology, Tokyo University of Science, 2641 Yamazaki, Noda 278-8510, Japan,* [∥]*Rigaku Corporation X-ray Research Laboratory, 3-9-12 Matsubaracho, Akishima, Tokyo 196-8666, Japan, and* [⊥]*Faculty of Science, Shizuoka University, 836 Ohya, Suruga-ku, Shizuoka 422-8529, Japan*

Received July 15, 2009

We previously reported on a 8-quinolinol-pendant cyclen ($L^5$) as a $Zn^{2+}$ fluorophore (cyclen = 1,4,7,10-tetraazacyclododecane) and its caged derivative, 8-(benzenesulfonyloxy)-5-(*N*,*N*-dimethylaminosulfonyl)quinolin-2-ylmethyl-pendant cyclen (BS-caged-$L^5$), which can be reactivated by hydrolysis of benzenesulfonyl group upon complexation with $Zn^{2+}$ at neutral pH to give a 1:1 $Zn^{2+}-L^5$ complex ($Zn(H_{-1}L^5)$). We report herein on the synthesis of 5,7-bis(*N*,*N*-dimethylaminosulfonyl)-8-hydroxyquinolin-2-ylmethyl-pendant cyclen ($L^6$) and its caged derivative (BS-caged-$L^6$) for more sensitive and more efficient cell-membrane permeability than those of $L^5$ and BS-caged-$L^5$. By potentiometric pH, $^1$H NMR, and UV−vis spectroscopic titrations, the deprotonation constants $pK_{a1}-pK_{a6}$ of $H_5L^6$ were determined to be <2, <2, <2, 2.5 ± 0.1 (for the 8-OH group of the quinoline moiety), 9.7 ± 0.1, and 10.8 ± 0.1 at 25 °C with $I$ = 0.1 ($NaNO_3$). The results of $^1$H NMR, potentiometric pH, UV−vis, and fluorescent titrations showed that $L^6$ rapidly forms a 1:1 complex with $Zn^{2+}$ ($Zn(H_{-1}L^6)$), the dissociation constant of which is 50 fM at pH 7.4. The fluorescent emission of $Zn(H_{-1}L^6)$ at 478 nm is 32 times as large as that of $L^6$ (excitation at 370 nm), and the fluorescent quantum yield of $Zn(H_{-1}L^6)$ ($\Phi_F$ = 0.41) is much greater than that of $Zn(H_{-1}L^5)$ ($\Phi_F$ = 0.044). The BS-caged-$L^6$ was reactivated by hydrolysis of the benzenesulfonyl moiety more rapidly (completes in 30 min at pH 7.4 at 37 °C) than BS-caged-$L^5$, presumably enabling the practical detection of $Zn^{2+}$ in sample solutions and living cells. The photochemical deprotection of BS-caged-$L^6$ and the cell membrane permeability of $L^6$ and BS-caged-$L^6$ are also described.

## Introduction

$Zn^{2+}$ is one of the indispensable metal ions in living systems, and its biological roles in $Zn^{2+}$ enzymes, DNA and RNA synthesis, gene expression, and so on have been extensively studied.[1] In recent years, a variety of additional functions of free $Zn^{2+}$ as a neural signal transmitter[2] and a key intracellular regulator of apoptosis[3] have been revealed. Therefore, the development of sensitive $Zn^{2+}$ sensors based

*To whom correspondence should be addressed. E-mail: shinaoki@rs.noda.tus.ac.jp.

(1) (a) Auld, D. A. In *Handbook of Metalloprotein*; Bertini, I., Sigel, A., Sigel, H., Eds.; Marcel Dekker: New York, 2001; pp 881−959. (b) Auld, D. S. *BioMetals* **2001**, *14*, 271–313. (c) Pabo, C. O.; Peisach, E.; Grant, R. A. *Annu. Rev. Biochem.* **2001**, *70*, 313–340. (d) Aoki, S.; Kimura, E. In *Comprehensive Coordination Chemistry II*; Que, L., Jr., Tolman, W. B., Eds.; Elsevier: Amsterdam, 2004; Vol. *8*, pp 601−640. (e) Maret, W. *J. Trace Elem. Med. Biol.* **2005**, *19*, 7–12. (f) Papworth, M.; Kolasinska, P.; Minczuk, M. *Gene* **2005**, *366*, 27–38. (g) Ye, B.; Maret, W.; Vallee, B. L. *Proc. Natl. Acad. Sci. U.S.A.* **2005**, *98*, 2317–2322.

(2) (a) Cuajungco, M. P.; Lees, G. J. *Neurobiol. Dis.* **1997**, *4*, 137–169. (b) Choi, D. W.; Koh, J. Y. *Annu. Rev. Neurosci.* **1998**, *21*, 347–375. (c) Frederickson, C. J.; Bush, A. I. *BioMetals* **2001**, *14*, 353–366. (d) Takeda, A. *BioMetals* **2001**, *14*, 343–351. (e) Burdette, S. C.; Lippard, S. J. *Coord. Chem. Rev.* **2001**, *216−217*, 333–361. (f) Burdette, S. C.; Lippard, S. J. *Proc. Natl. Acad. Sci. U.S.A.* **2003**, *100*, 3605–3610.

(3) (a) Treves, S.; Trentini, P. L.; Ascannelli, M.; Bucci, G.; Di Virgilio, F. *Exp. Cell Res.* **1994**, *211*, 339–343. (b) Perry, D. K.; Smyth, M. J.; Stennicke, H. R.; Salvesen, G. S.; Duriez, P.; Poirier, G. G.; Hannun, Y. A. *J. Biol. Chem.* **1997**, *272*, 18530–18533. (c) Chai, F.; Truong-Tran, A. Q.; Ho, L. H.; Zalewski, P. D. *Immuno. Cell. Biol.* **1999**, *77*, 272–278. (d) Truong-Tran, A. Q.; Carter, J.; Ruffin, R. E.; Zalewski, P. D. *BioMetals* **2001**, *14*, 315–330.


Published on Web 12/29/2009

**Scheme 1**

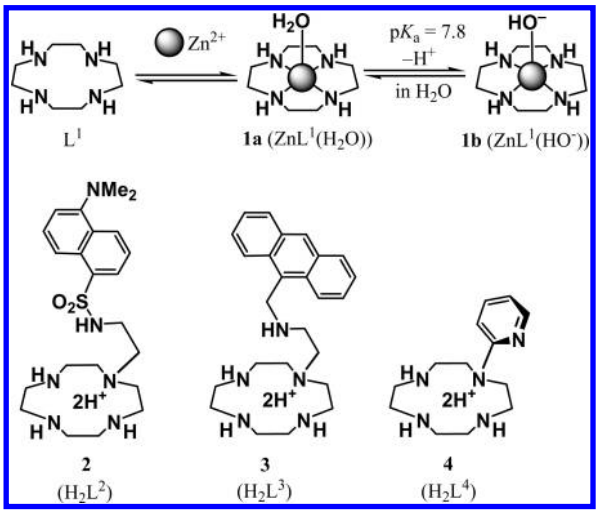


on chelation-enhanced fluorescent mechanisms is currently of great interest.[4,5]

It has been established that 1,4,7,10-tetraazacyclododecane (cyclen, $L^1$) forms a very stable $Zn^{2+}$ complex **1** ($ZnL^1$)[6] in aqueous solution at neutral pH (Scheme 1) and is a potential platform for $Zn^{2+}$-selective fluorophores[4a,c] such as **2** ($L^2$),[7] **3** ($L^3$),[8] **4** ($L^4$).[9]

We recently reported on a $Zn^{2+}$ fluorophore **5** ($L^5$)[10] bearing 5-*N*,*N*-dimethylamino-8-hydroxyquinoline and cyclen moieties (Scheme 2). The fluorescent emission of **5** increased by a factor of 22 upon complexation with $Zn^{2+}$ (quantum yields ($\Phi_F$) for the emission of **5** and **6** are $2.0 \times 10^{-3}$ and $4.4 \times 10^{-2}$). In addition, it was found that **5** forms a very stable $Zn^{2+}$ complex **6** ($Zn(H_{-1}L^5)$) in aqueous solution

**Scheme 2**

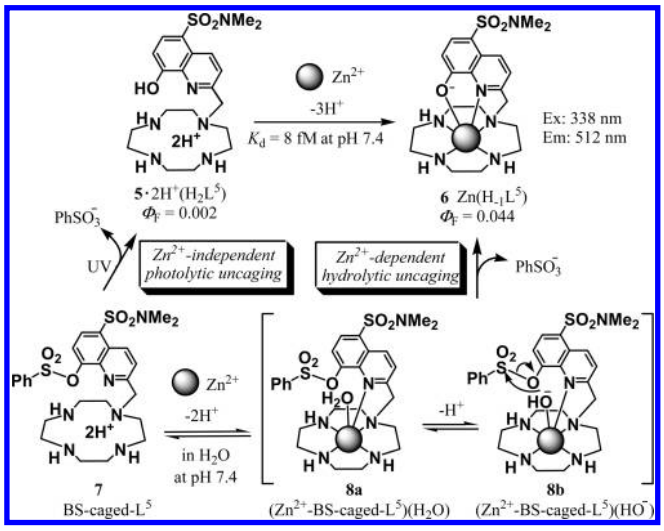


($K_d$ = 8 fM at pH 7.4) and that its $Zn^{2+}$ complexation is complete in the order of milliseconds. A "caged (chemically protected)" derivative of **5**, **7** (BS-caged-$L^5$), was recently synthesized, in attempts to improve $Zn^{2+}/Cd^{2+}$ selectivity and cell-membrane permeability (Scheme 2).[11] It was found that **7** forms a $Zn^{2+}$ complex **8** ($Zn^{2+}$-BS-caged-$L^5$) and that the $Zn^{2+}$-bound $H_2O$ in **8a** was deprotonated to afford $Zn^{2+}-HO^-$ species (**8b**), which promoted the hydrolysis of the benzenesulfonyl group, resulting in the formation of **6** ($Zn(H_{-1}L^5)$) ($Zn^{2+}$-dependent hydrolytic uncaging). While $Zn^{2+}/Cd^{2+}$ selectivity was not improved, considerable enhancement in cellular uptake was achieved. In addition, we happened to find that the photoirradiation of **7** promotes the photochemical hydrolysis of its sulfonate moiety to yield **5** and benzenesulfonate ($PhSO_3^-$) in the absence and presence of $Zn^{2+}$ ($Zn^{2+}$-independent photolytic uncaging).

In this work, we wish to report on the synthesis of 5,7-bis(*N*,*N*-dimethylaminosulfonyl)-8-hydroxyquinolin-2-ylmethyl-pendant cyclen **10** ($L^6$) (Scheme 3). It had previously been reported that 5,7-bis(*N*,*N*-dimethylaminosulfonyl)-2-methyl-8-quinolinol **9b** has a much greater quantum yield for emission ($\Phi_F$ = 0.70) than that ($\Phi_F$ = 0.24) of **9a**.[12] Therefore, it was expected that **10** ($L^6$) would be a more sensitive $Zn^{2+}$ probe than **5** ($L^5$). In this manuscript, we describe the chemical and photochemical behaviors of **10** and the $Zn^{2+}$-dependent hydrolytic and $Zn^{2+}$-independent photochemical reactions of the caged derivative **12** (BS-caged-$L^6$). Data on the intracellular concentrations of **10** and **12** and the staining of $Zn^{2+}$-loaded living cells with these probes are also presented.

## Experimental Section

**General Information.** Reagents and solvents were purchased at the highest commercial quality and were used without further purification. *N*-bromosuccinimide (NBS) was recrystallized from water before use. $ZnSO_4 \cdot 7H_2O$, $Zn(NO_3)_2 \cdot 6H_2O$, $3CdSO_4 \cdot 8H_2O$, $CuSO_4 \cdot 5H_2O$, $CoSO_4 \cdot 7H_2O$, $FeSO_4 \cdot 7H_2O$, $AgNO_3$, $FeCl_3 \cdot 6H_2O$, KCl, $MgSO_4$, and $CaSO_4 \cdot 2H_2O$ were

(4) Reviews: (a) Kimura, E.; Koike, T. *Chem. Soc. Rev.* **1998**, *27*, 179–184. (b) Prodi, L.; Bolletta, F.; Montalti, M.; Zaccheroni, N. *Coord. Chem. Rev.* **2000**, *205*, 59–83. (c) Kimura, E.; Aoki, S. *BioMetals.* **2001**, *14*, 191–204. (d) Kikuchi, K.; Komatsu, K.; Nagano, T. *Curr. Opin. Chem. Biol.* **2004**, *8*, 182–191. (e) Jiang, P.; Guo, Z. *Coord. Chem. Rev.* **2004**, *248*, 205–229. (f) Dai, Z.; Canary, J. W. *New J. Chem.* **2007**, *31*, 1708–1718. (g) Nolan, E. M.; Lippard, S. J. *Acc. Chem. Res.* **2009**, *42*, 193–203.

(5) For recent examples, see: (a) Burdette, S. C.; Lippard, S. J. *Proc. Natl. Acad. Sci. U.S.A.* **2003**, *100*, 3605–3610. (b) Woodroofe, C. C.; Masalha, R.; Barnes, K. R.; Frederickson, C. J.; Lippard, S. J. *Chem. Biol.* **2004**, *11*, 1659–1666. (c) Kiyose, K.; Kojima, H.; Urano, Y.; Nagano, T. *J. Am. Chem. Soc.* **2006**, *128*, 6548–6549. (d) Harriman, A.; Mallon, L. J.; Stewart, B.; Ulrich, G.; Ziessel, R. *Eur. J. Org. Chem.* **2007**, 3191–3198. (e) Parkesh, R.; Lee, T. C.; Gunnlaugsson, T. *Org. Biomol. Chem.* **2007**, *5*, 310–317. (f) Atilgan, S.; Ozdemir, T.; Akkaya, E. U. *Org. Lett.* **2008**, *10*, 4065–4067. (g) Zhang, Y.; Guo, X.; Si, W.; Jia, L.; Qian, X. *Org. Lett.* **2008**, *10*, 473–476. (h) Alarcón, J.; Albelda, M. T.; Belda, R.; Clares, M. P.; Delgado-Pinar, E.; Frías, J. C.; García-España, E.; González, J.; Soriano, C. *Dalton Trans.* **2008**, 6530–6538. (i) Qian, F.; Zhang, C.; Zhang, Y.; He, W.; Gao, X.; Hu, P.; Guo, Z. *J. Am. Chem. Soc.* **2009**, *131*, 1460–1468. (j) Tamanini, E.; Katewa, A.; Sedger, L. M.; Todd, M. H.; Watkinson, M. *Inorg. Chem.* **2009**, *48*, 319–324.

(6) (a) Kimura, E.; Shiota, T.; Koike, T.; Shiro, M.; Kodama, M. *J. Am. Chem. Soc.* **1990**, *112*, 5805–5811. (b) Kimura, E.; Shionoya, M.; Hoshino, A.; Ikeda, T.; Yamada, Y. *J. Am. Chem. Soc.* **1992**, *114*, 10134–10137.

(7) (a) Koike, T.; Watanabe, T.; Aoki, S.; Kimura, E.; Shiro, M. *J. Am. Chem. Soc.* **1996**, *118*, 12696–12703. (b) Kimura, E.; Koike, T. *Chem. Soc. Rev.* **1998**, *27*, 179–184. (c) Kimura, E.; Aoki, S.; Kikuta, E.; Koike, T. *Proc. Natl. Acad. Sci. U.S.A.* **2003**, *100*, 3731–3736. (d) Kimura, E.; Takasawa, R.; Tanuma, S.; Aoki, S. *Science STKE* **2004**, *223*, 7.

(8) Aoki, S.; Kaido, S.; Fujioka, H.; Kimura, E. *Inorg. Chem.* **2003**, *42*, 1023–1030.

(9) Aoki, S.; Kagata, D.; Shiro, M.; Takeda, K.; Kimura, E. *J. Am. Chem. Soc.* **2004**, *126*, 13377–13390.

(10) Aoki, S.; Sakurama, K.; Matsuo, N.; Yamada, Y.; Takasawa, R.; Tanuma, S.; Shiro, M.; Takeda, K.; Kimura, E. *Chem.—Eur. J.* **2006**, *12*, 9066–9080.

(11) Aoki, S.; Sakurama, K.; Ohshima, R.; Matsuo, N.; Yamada, Y.; Takasawa, R.; Tanuma, S.; Takeda, K.; Kimura, E. *Inorg. Chem.* **2008**, *47*, 2747–2754.

(12) Pearce, D. A.; Jotterand, N.; Carrico, I. S.; Imperiali, B. *J. Am. Chem. Soc.* **2001**, *123*, 5160–5161.

**Scheme 3**

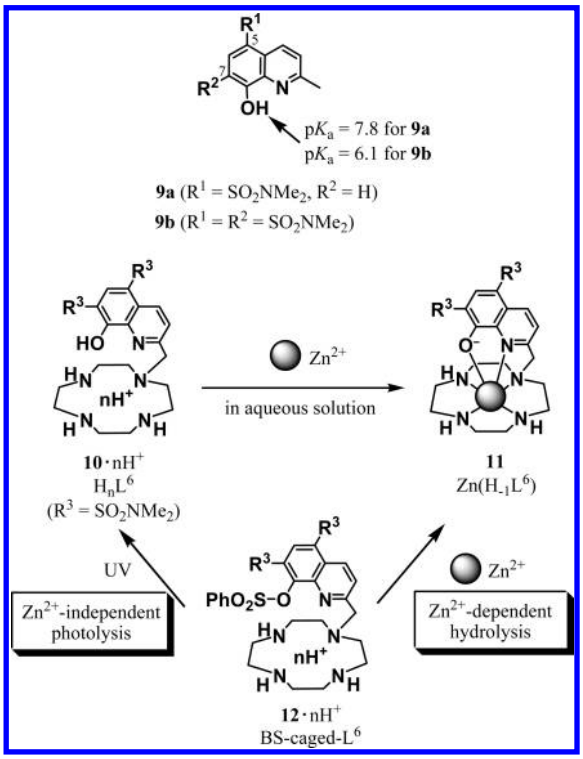


purchased from Kanto Chemical Co. Ltd.; HgCl was purchased from Yoneyama Kogyo Co.; $Al(NO_3)_3 \cdot 9H_2O$ and $MnSO_4 \cdot H_2O$ were purchased from Sigma-Aldrich Chemical Co.; $Eu(NO_3)_3 \cdot 6H_2O$ and $Y(NO_3)_3 \cdot 6H_2O$ were purchased from Soekawa Co. All aqueous solutions were prepared using deionized and distilled water. Buffer solutions (CAPS, pH 13.0, 12.0, 11.0 and 10.0; CHES, pH 9.0; TAPS, pH 8.0; HEPES, pH 7.4, and 7.0; MES, pH 6.0; acetic acid/sodium acetate, pH 5.0 and 4.0; Gly/HCl, pH 3.0; KCl/HCl, pH 2.0 and 1.0) were used, and the ionic strengths were adjusted with $NaNO_3$. The Good's buffer reagents (Dojindo) were obtained from commercial sources: MES (2-morpholinoethanesulfonic acid, $pK_a$ = 4.8), HEPES (*N*-(2-hydroxyethyl)piperazine-*N*′-2-ethanesulfonic acid, $pK_a$ = 7.5), TAPS (*N*-[tris(hydroxymethyl)methylamino]-3-propanesulfonic acid, $pK_a$ = 8.4), CHES (2-(cyclohexylamino)-ethanesulfonic acid, $pK_a$ = 9.5), CAPS (3-(cyclohexylamino)-propanesulfonic acid, $pK_a$ = 10.4). Melting points were measured on a Büchi 510 Melting Point Apparatus and are uncorrected. UV−vis spectra were recorded on a JASCO UV/vis spectrophotometer V-550, and fluorescence (excitation and emission) spectra were recorded on JASCO FP-6200 and FP-6500 spectrofluorometers at 25.0 ± 0.1 °C. The quantum yields ($\Phi_F$) for fluorescence emission were determined by comparison with the integrated corrected emission spectrum of quinine sulfate (a standard), whose quantum yield in 0.1 M $H_2SO_4$ was assumed to be 0.55 (excitation at 366 nm).[13] IR spectra were recorded on a JASCO FTIR-410 spectrophotometer at room temperature. $^1$H (300 MHz) and $^{13}$C (75 MHz) NMR spectra were recorded on a JEOL Always 300 spectrometer. Tetramethylsilane was used as an internal reference for $^1$H and $CDCl_3$ for $^{13}$C NMR measurements in $CDCl_3$. 3-(Trimethylsilyl)-propionic-2,2,3,3-$d_4$ acid (TSP) sodium salt was used as an external reference for $^1$H and 1,4-dioxane for $^{13}$C NMR measurements in $D_2O$. The pD values in $D_2O$ were corrected for a deuterium isotope effect using pD = (pH-meter reading) + 0.40. MS measurements were performed on a JEOL JMS-SX-102A. Elemental analyses were performed on a Perkin-Elmer CHN 2400 analyzer. Thin-layer (TLC) and silica gel column chromatographies were performed using a Merck Silica gel 60 $F_{254}$ TLC plate and Fuji Silysia Chemical FL-100D, respectively.

**8-(Benzenesulfonyloxy)-5,7-bis(*N*,*N*-dimethylaminosulfonyl)-quinaldine (13).** Benzenesulfonyl chloride (1.2 g, 6.9 mmol) and 4-dimethylaminopyridine (126 mg, 1.0 mmol) were added to a solution of 5,7-bis(*N*,*N*-dimethylaminosulfonyl)-8-hydroxyquinaldine **9b**[12] (1.3 g, 3.4 mmol) and $Et_3N$ (630 μL, 4.5 mmol) in $CH_2Cl_2$ (30 mL) at 0 °C, and the resulting solution was stirred at reflux temperature for 1 day. The reaction mixture was concentrated under reduced pressure, and the resulting residue was purified by silica gel column chromatography (hexane/AcOEt = 3:1); recrystallization from AcOEt afforded **13** as colorless prisms (1.3 g, 74% yield). The starting material **9b** was recovered (199 mg, 16% yield). mp. 176−178 °C. $^1$H NMR (300 MHz, $CDCl_3$/TMS): δ 2.40 (s, 3H), 2.82 (s, 6H), 2.91 (s, 6H), 7.49 (d, *J* = 9.0 Hz, 1H), 7.62 (t, *J* = 8.4 Hz, 2H), 7.74 (t, *J* = 8.4 Hz, 1H), 8.06 (d, *J* = 8.4 Hz, 2H), 8.53 (s, 1H), 9.00 ppm (d, *J* = 9.0 Hz, 1H). $^{13}$C NMR (75 MHz, $CDCl_3$/TMS): δ 24.8, 37.6, 125.9, 126.6, 128.1, 128.4, 128.8, 130.1, 132.2, 133.6, 133.8, 139.0, 142.2, 148.2, 161.5 ppm. IR (KBr pellet): 3098, 3065, 2975, 2923, 1609, 1586, 1548, 1495, 1450, 1372, 1345, 1284, 1245, 1181, 1165, 1144, 1075, 1033, 968, 835, 797, 764, 718, 689, 654, 625, 607, 587, 557, 509, 490, 438 $cm^{-1}$. Elemental analysis: calcd for $C_{20}H_{23}N_3O_7S_3$ (513.61): C, 46.77; H, 4.51; N, 8.18; found: C, 46.77; H, 4.18; N, 8.16.

**8-(Benzenesulfonyloxy)-5,7-bis(*N*,*N*-dimethylaminosulfonyl)-2-(bromomethyl)quinoline (14).** A mixture of **13** (300 mg, 0.6 mmol), *N*-bromosuccinimide (84 mg, 0.5 mmol) and AIBN (20 mg, 0.1 mmol) in distilled $CCl_4$ (20 mL) was stirred at reflux temperature for 3 h (the *N*-bromosuccinimide was added portionwise), and the reaction mixture was concentrated under reduced pressure. The residue was dissolved in $CH_2Cl_2$ (5 mL) and washed with a saturated solution of $Na_2CO_3$ and $Na_2S_2O_4$. The organic layer was dried over anhydrous $Na_2SO_4$, filtered, and concentrated under reduced pressure. The resulting residue was purified by silica gel column chromatography (hexane/AcOEt = 2:1) to afford **14** as a colorless amorphous solid (52 mg, 15% yield). The starting material **13** was recovered in 58% yield (175 mg). $^1$H NMR (300 MHz, $CDCl_3$/TMS): δ 2.87 (s, 6H), 2.92 (s, 6H), 4.08 (s, 2H), 7.66 (t, *J* = 7.8 Hz, 2H), 7.78 (t, *J* = 7.8 Hz, 1H), 7.80 (d, *J* = 9.0 Hz, 1H), 8.06 (d, *J* = 7.5 Hz, 2H), 8.61 (s, 1H), 9.13 ppm (d, *J* = 9.0 Hz, 1H). $^{13}$C NMR (75 MHz, $CDCl_3$/TMS): δ 32.3, 37.6, 125.2, 127.2, 128.3, 129.0, 129.4, 131.1, 132.5, 133.9, 135.1, 139.0, 141.7, 148.4, 159.0 ppm. IR (KBr pellet): 3098, 2967, 2921, 1542, 1495, 1450, 1384, 1495, 1349, 1290, 1196, 1177, 1146, 1069, 961, 798, 769, 725, 688, 669, 607, 583, 551 $cm^{-1}$. HRMS (FAB+): calcd for $[M+H]^+$, 591.9881; found, 591.9879.

**1-[8-(Benzenesulfonyloxy)-5,7-bis(*N*,*N*-dimethylaminosulfonyl)-quinolin-2-ylmethyl]-4,7,10-tris(*tert*-butyloxycarbonyl)-1,4,7,10-tetraazacyclododecane (16).** A mixture of 3Boc-cyclen **15**[14] (131 mg, 0.28 mmol), **14** (180 mg, 0.30 mmol) and $Na_2CO_3$ (50 mg, 0.47 mmol) in $CH_3CN$ (20 mL) was stirred at 60 °C overnight under an argon atmosphere. After removing the insoluble inorganic salts by filtration, the filtrate was concentrated under reduced pressure. The resulting residue was purified by silica gel column chromatography ($CH_2Cl_2$/MeOH = 100:1) to afford **16** as a pale yellow amorphous solid (246 mg, 90% yield). $^1$H NMR (300 MHz, $CDCl_3$/TMS): δ 1.43−1.48 (m, 27H), 2.73 (s, 6H), 2.90 (s, 6H), 2.73−3.57 (br, 16H), 3.86 (s, 2H), 7.61 (t, *J* = 7.5 Hz, 2H), 7.74 (t, *J* = 7.5 Hz, 1H), 7.81 (d, *J* = 9.0 Hz, 1H), 8.04 (d, *J* = 7.5 Hz, 2H), 8.55 (s, 1H), 9.02 ppm (d, *J* = 9.0 Hz, 1H). $^{13}$C NMR (75 MHz, $CDCl_3$/TMS): δ 19.2, 27.1, 28.3, 28.5, 35.1,

(13) (a) Turro, N. J. *Modern Molecular Photochemistry*; University Science Books: Sausalito, CA, 1991. (b) Murov, S. L.; Carmichael, I.; Hug, G. L. *Handbook of Photochemistry*, 2nd ed.; Marcel Dekker: New York, 1993.

(14) Kimura, E.; Aoki, S.; Koike, T.; Shiro, M. *J. Am. Chem. Soc.* **1997**, *119*, 3068–3076.

37.4, 46.1, 47.7, 49.9, 50.6, 54.3, 55.2, 58.1, 79.5, 125.9, 127.2, 128.5, 128.6, 128.8, 129.2, 132.0, 133.3, 134.0, 138.3, 142.0, 148.5, 155.7, 176.4 ppm. IR (KBr pellet): 2974, 2931, 2815, 1689, 1597, 1560, 1458, 1415, 1365, 1342, 1250, 1152, 1049, 962, 859, 774, 725, 622, 556 $cm^{-1}$. HRMS (FAB+): calcd for $[M+H]^+$, 984.3881; found, 984.3881.

**1-[5,7-Bis(*N*,*N*-dimethylaminosulfonyl)-8-hydroxyquinolin-2-ylmethyl]-4,7,10-tris(*tert*-butyloxycarbonyl)-1,4,7,10-tetraazacyclododecane (17).** One N aq. NaOH (1 mL) was added to a solution of **16** (80 mg, 0.081 mmol) in MeOH (5 mL) at room temperature, and the mixture was stirred at reflux temperature for 3 h. After cooling, the reaction mixture was concentrated under reduced pressure and purified by silica gel column chromatography ($CH_2Cl_2$/MeOH = 100:1) to afford **17** as a colorless powder (64 mg, 93% yield). mp. 95−98 °C. $^1$H NMR (300 MHz, $CDCl_3$/TMS): $\delta$ 1.42−1.49 (m, 27H), 2.81 (s, 6H), 2.95 (s, 6H), 2.81−3.61 (m, 16H), 4.14 (s, 2H), 7.83 (d, $J$ = 9.0 Hz, 1H), 8.50 (s, 1H), 9.02 ppm (d, $J$ = 9.0 Hz, 1H). $^{13}$C NMR (75 MHz, $CDCl_3$/TMS): $\delta$ 20.6, 22.6, 25.2, 28.4, 28.6, 31.5, 34.6, 37.4, 37.7, 47.4, 49.9, 54.5, 57.6, 79.7, 117.7, 122.9, 125.9, 126.3, 130.9, 134.8, 137.7, 154.6 ppm. IR (KBr pellet): 3447, 2974, 2931, 2815, 1689, 1597, 1560, 1458, 1415, 1365, 1250, 1152, 962, 859, 774, 725, 622, 556 $cm^{-1}$. HRMS (FAB−): calcd for $[M-H]^-$, 842.3792; found, 842.3793.

**1-[5,7-Bis(*N*,*N*-dimethylaminosulfonyl)-8-hydroxyquinolin-2-ylmethyl]-1,4,7,10-tetraazacyclododecane Trihydrochloride Salt (10·3HCl·H$_2$O).** Conc. HCl (1 mL) was added dropwise to a solution of **17** (290 mg, 0.34 mmol) in MeOH (5 mL), and the resulting solution was stirred at 70 °C for 10 min. The reaction mixture was concentrated under reduced pressure, azeotroped with $CHCl_3$, and the resulting solid was recrystallized from $H_2O$/EtOH to afford **10**·3HCl salt (characterized by elemental analysis and potentiometric pH titration) as a colorless powder (170 mg, 74% yield). After concentrating the filtrate under reduced pressure, a green powder was obtained, which was characterized as the **10**·4HCl salt (26 mg, 11% yield) by elemental analysis.[15]

For the **10**·3HCl salt: mp. > 250 °C. $^1$H NMR (300 MHz, $D_2O$/external TSP): $\delta$ 2.81 (s, 6H), 2.89 (s, 6H), 3.05−3.25 (m, 16H), 4.22 (s, 2H), 7.75 (d, $J$ = 9.0 Hz, 1H), 8.34 (s, 1H), 8.94 ppm (d, $J$ = 9.0 Hz, 1H). $^{13}$C NMR (75 MHz, $D_2O$/external 1,4-dioxane): $\delta$ 36.8, 37.2, 41.7, 42.5, 42.9, 48.6, 57.0, 115.4, 119.9, 126.5, 130.6, 135.4, 138.3, 156.5, 156.7 ppm. IR (KBr pellet): 3423, 2961, 1595, 1560, 1499, 1456, 1336, 1145, 1099, 1072, 955, 848, 787, 727, 622, 557 $cm^{-1}$. Elemental analysis: calcd for $C_{22}H_{42}Cl_3N_7O_6S_2$ (671.10): C, 39.37; H, 6.31; N, 14.61; found: C, 39.43; H, 6.39; N, 14.42.

For the **10**·4HCl salt: mp. 248−251 °C (decomp.). Elemental analysis: calcd for $C_{22}H_{41}Cl_4N_7O_5S_2$ (689.55): C, 38.32; H, 5.99; N, 14.22; found: C, 38.47; H, 6.28; N, 13.99.

**1-[8-(Benzenesulfonyloxy)-5,7-bis(*N*,*N*-dimethylaminosulfonyl)quinolin-2-ylmethyl]-1,4,7,10-tetraazacyclododecane 3TFA Salt (12·3TFA·0.5H$_2$O).** A solution of trifluoroacetic acid (1.5 mL, 5.2 mmol) in $CH_2Cl_2$ (2.5 mL) was added to a solution of **16** (200 mg, 0.20 mmol) in $CH_2Cl_2$ (2.5 mL), and the resulting solution was stirred at 60 °C for 0.5 h. The reaction mixture was concentrated under reduced pressure, azeotroped with $CHCl_3$, and the resulting residue was recrystallized from $Et_2O$/EtOH to afford a **12**·3TFA salt (12·3TFA·0.5$H_2O$) as a colorless powder (177 mg, 84% yield). mp. > 250 °C. $^1$H NMR (300 MHz, $D_2O$/external TSP): $\delta$ 2.73 (s, 6H), 2.88 (s, 6H), 2.98−3.30 (m, 16H), 4.13 (s, 2H), 7.70 (t, $J$ = 7.8 Hz, 2H), 7.89 (t, $J$ = 7.8 Hz, 1H), 7.94−8.01 (m, 3H), 8.42 (s, 1H), 9.21 ppm (d, $J$ = 9.0 Hz, 1H). $^{13}$C NMR (75 MHz, $D_2O$/external 1,4-dioxane): $\delta$ 36.6, 36.8, 41.2, 41.6, 44.2, 47.7, 57.8, 126.8, 127.3, 127.7, 128.3, 129.1, 131.0, 134.5, 135.2, 135.4, 142.2, 147.6, 149.9, 159.8, 162.2, 162.6 ppm. IR (KBr pellet): 3411, 2923, 2851, 1682, 1550, 1454, 1347, 1202, 1142, 1071, 962, 835, 799, 722, 688, 607, 585, 556 $cm^{-1}$. Elemental analysis: calcd for $C_{34}H_{45}F_9N_7O_{13.5}S_3$ (1034.94): C, 39.46; H, 4.38; N, 9.47; found: C, 39.67; H, 4.63; N, 9.67.

**1-[5,7-Bis(*N*,*N*-dimethylaminosulfonyl)-8-hydroxyquinolin-2-ylmethyl]-1,4,7,10-tetraazacyclododecane Zn(NO$_3$) Complex (11·NO$_3$·1.3H$_2$O).** A solution of $Zn(NO_3)_2\cdot 6H_2O$ (15 mg, 0.05 mmol) in water (1 mL) was added into a solution of **10**·3HCl·$H_2O$ (34 mg, 0.05 mmol) in $H_2O$ (3 mL), and the pH of a reaction mixture adjusted to 10.0 by adding aq. NaOH. After the insoluble compounds were removed by filtration, the filtrate was slowly concentrated at atmospheric pressure to obtain **11**·$NO_3\cdot 1.3H_2O$ as colorless prisms (8 mg, 23% yield). mp. > 250 °C. $^1$H NMR (300 MHz, $D_2O$/external TSP): $\delta$ 2.74 (s, 6H), 2.86 (s, 6H), 2.91−3.20 (m, 16H), 4.34 (s, 2H), 7.74 (d, $J$ = 8.7 Hz, 1H), 8.27 (s, 1H), 8.94 ppm (d, $J$ = 8.7 Hz, 1H). $^{13}$C NMR (75 MHz, DMSO/TMS): $\delta$ 37.0, 38.0, 43.6, 44.2, 45.0, 52.5, 57.5, 108.6, 116.0, 123.9, 126.7, 134.9, 136.8, 140.3, 155.4, 166.1 ppm. IR (KBr pellet): 3570, 3448, 3332, 3273, 2928, 2879, 1649, 1548, 1508, 1488, 1385, 1316, 1283, 1259, 1198, 1167, 1140, 1119, 1092, 1042, 993, 950, 930, 853, 796, 750, 720, 688, 596, 560 $cm^{-1}$. Elemental analysis: calcd for $C_{22}H_{36.6}N_8O_{9.3}S_2Zn$ (691.49): C, 38.21; H, 5.33; N, 16.20; found: C, 37.83; H, 5.21; N, 16.00.

**Potentiometric pH Titrations.** The preparation of the test solutions and the calibration method of the electrode system (Potentiometric Automatic Titrator AT-400 and Auto Piston Buret APB-410, Kyoto Electronics Manufacturing, Co. Ltd. with a Kyoto Electronics Manufacturing Co. Combination pH Electrode 98100C171) have been described in earlier reports.[10,11] All test solutions (50 mL) were stored under an argon atmosphere. Potentiometric pH titrations were performed with $I$ = 0.1 ($NaNO_3$) at 25 ± 0.1 °C. The deprotonation constants of $Zn^{2+}$-bound water $K_2'$ (= [$HO^-$-bound species][$H^+$]/[$H_2O$-bound species]) were determined by means of the "BEST" software program.[16] The $K_w$ (equivalent to $a_{H+}a_{OH-}$), $K_w'$ (equivalent to [$H^+$][$HO^-$]), $f_{H+}$ values used at 25 °C were $10^{-14.00}$, $10^{-13.79}$, and 0.825, respectively. The corresponding mixed constants $K_2$ (= [$HO^-$-bound species]$a_{H+}$/[$H_2O$-bound species]), were derived by using $[H^+] = a_{H+}/f_{H+}$. The percentage species distribution values against pH (= $-\log [H^+] + 0.084$) were obtained using the SPE software program.[16]

**Crystallographic Study of 10 ($H_2(H_{-1}L^6)$ (= $HL^6$)). 10** ($H_2(H_{-1}L^6)$ (= $HL^6$)) was recrystallized from an aqueous solution of **10** at pH 5 and 4 °C. These crystals, which were filtered and dried, were determined to be $[HL^6]^+\cdot Cl^-\cdot 4.2H_2O$ by elemental analysis (Anal. Calcd for $C_{22}H_{38}Cl_1N_7O_5S_2\cdot 4.2H_2O$: C 40.29, H 7.13, N 14.95. Found: C 39.85, H 6.68, N 14.61). All measurements were made on a Rigaku RAXIS-RAPID instrument with graphite monochromated Cu Kα radiation at 93 K. The structure was solved by direct methods[17] and refined by full-matrix least-squares techniques. All calculations were performed using the CrystalStructure crystallographic software package except for refinements, which were performed with SHELXL-97.[18] $C_{22}H_{50.4}Cl_1N_7O_{11.2}S_2$, $M_r$ = 691.85, a colorless block crystal, crystal size 0.15 × 0.14 × 0.14 mm, monoclinic, space group $C2/c$ (#15), $a$ = 35.8779(7), $b$ = 19.7401(4), $c$ = 21.4880(7) Å, $\beta$ = 118.8100(7)°, $V$ = 13334.9(6) Å$^3$, $Z$ = 16, $D_{calc}$ = 1.378 g·cm$^{-3}$, 91503 measured reflections, 11999 unique reflections, $2\theta_{max}$ = 68.3°, $R1$ (w$R2$) = 0.0685

(15) As described in the Experimental Section, 3HCl and 4HCl salt of **10** were obtained as colorless and green powders, respectively. As pointed out by the reviewer, this may be related to the protonation status of both salts in the solid state, although we do not have experimental evidence.

(16) Martell, A. E.; Motekaitis, R. J. *Determination and Use of Stability Constants*, 2nd ed.; VCH: New York, 1992.

(17) Burla, M. C.; Caliandro, R.; Camalli, M.; Carrozzini, B.; Cascarano, G. L.; De Caro, L.; Giacovazzo, C.; Polidori, G.; Spagna, R. *J. Appl. Crystallogr.* **2005**, *38*, 381–388.

(18) Sheldrick, G. M. *SHELX-97, Program for the Refinement of Crystal Structures*; University of Göttingen: Göttingen, Germany, 1997.

**Scheme 4**

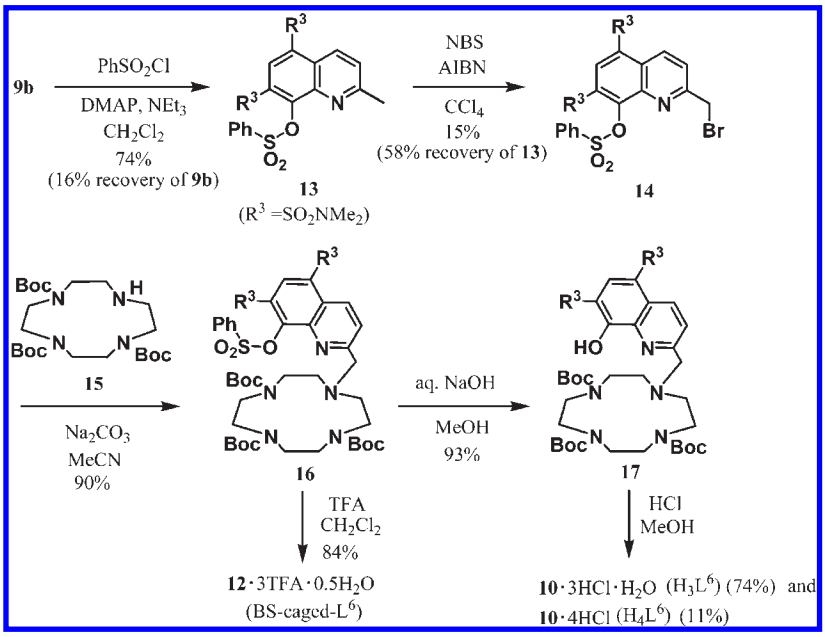


(0.1966), GOF = 1.033. Full details of the crystallographic analysis of **10** are given in the Supporting Information.

**Crystallographic Study of 11·NO$_3$ (Zn(H$_{-1}$L$^6$)·NO$_3$).** **11**·NO$_3$ (Zn(H$_{-1}$L$^6$)·NO$_3$) was recrystallized by the slow evaporation of an aqueous solution. All measurements were made on a Rigaku Saturn CCD area detector with graphite monochromated Mo Kα radiation at 133 K. $C_{22}H_{36}N_8O_9S_2Zn$, $M_r$ = 686.07, a colorless block crystal, crystal size 0.25 × 0.20 × 0.15 mm, monoclinic, space group $P2_1/n$ (#14), $a$ = 11.602(5), $b$ = 13.792(6), $c$ = 17.941(8) Å, $\beta$ = 93.923(3)°, $V$ = 2864(2) Å$^3$, $Z$ = 4, $D_{calc}$ = 1.591 g cm$^{-3}$, 22048 measured reflections, 7339 unique reflections, $2\theta_{max}$ = 57.4°, $R1$ (w$R2$) = 0.0646 (0.1901), GOF = 0.999. Full details of crystallographic analysis of **11**·NO$_3$ are given in the Supporting Information.

**Photoreaction.** Sample solutions were prepared in quartz cuvettes (GL Science Inc. Japan, 10 mm light path) and irradiated at a wavelength 328 or 330 nm on JASCO FP-6200 or those of FP-6500 spectrofluorometer. The photoreactions were followed by UV−vis (50 μM) spectra or $^1$H NMR spectra. The averaged light intensities of the JASCO FP-6200 spectrofluorometer at 330 nm were determined to be 1.4 × 10$^{-5}$ mol·sec$^{-1}$ (slit width for excitation = 20 nm), and those of the JASCO FP-6500 spectrofluorometer at 328 nm were determined to be 5.3 × 10$^{-6}$ mol·sec$^{-1}$ (slit width for excitation = 20 nm) relative to the potassium ferioxalate actinometer.[13] The reactions were repeated two or three times, and the averaged values were calculated. Experimental fluctuations were ± 5%.

**Treatment of HeLa Cells with Zn$^{2+}$ Probes and Fluorescence Microscopy.** HeLa cells were seeded onto 35 mm glass-bottom dishes. The cells were incubated with Zn$^{2+}$ fluorophores **10** and **12** (50 μM) in culture medium for 0.5 h in a humid atmosphere of 5% $CO_2$ at 37 °C, then washed twice with PBS, and the culture medium (2 mL) was replaced. The cells were treated with 25 μM $ZnSO_4 \cdot 7H_2O$ and 20 μM pyrithione for 10 min, washed with PBS and observed by phase contrast and fluorescence microscopy (KEYENCE fluorescent microscope, BZ-9000; excitation at 360/40 nm, emission 460/50 nm).

## Results and Discussion

**Synthesis of Zn$^{2+}$ Fluorophores 10 and 12 (L$^6$ and BS-caged-L$^6$).** A ligand **10** (L$^6$) and its benzenesulfonyl-caged derivative **12** (BS-caged-L$^6$) were synthesized as shown in Scheme 4. The reaction of **9b**[12] with benzenesulfonyl chloride in the presence of 4-dimethylaminopyridine (DMAP) and $Et_3N$ in $CH_2Cl_2$ gave **13**, the 2-methyl group of which was brominated with NBS and AIBN in $CCl_4$ to give **14**. The reaction of **14** with 3Boc-cyclen **15**[14] gave **16**, the three Boc groups of which were deprotected with trifluoroacetic acid (TFA) in $CH_2Cl_2$ afforded **12** (BS-caged-L$^6$) as the 3TFA salt. The $PhSO_2$ group of **16** was removed by treatment with aqueous NaOH to give **17**, the Boc groups of which were deprotected by treatment with HCl in MeOH afforded **10** (L$^6$). It should be noted that **10** was obtained as a colorless powder, and concentration of its filtrate gave a green powder. These two powders were determined to be 3HCl salt (**10**·3HCl·$H_2O$) and 4HCl salt (**10**·4HCl), respectively, by elemental analysis and potentiometric pH titrations.[15]

**Deprotonation Constants for 10 (L$^6$) Determined by Potentiometric pH Titration, $^1$H NMR, and UV−vis Spectra.** A typical potentiometric pH titration curve for 1 mM **10**·3HCl·$H_2O$ ($H_3L^6$) + 2 mM $HNO_3$ against aqueous 0.1 M NaOH with $I$ = 0.1 ($NaNO_3$) at 25 °C (dashed curve (a) in Figure 1) was analyzed for acid−base equilibrium (1). The deprotonation constants p$K_{ai}$ ($i$ = 1−6) of $H_5L^6$ were determined to be < 2 (p$K_{a1}$∼p$K_{a3}$), 2.5 ± 0.1 (p$K_{a4}$), 9.7 ± 0.1 (p$K_{a5}$), and 10.8 ± 0.1 (p$K_{a6}$) (Table 1) by using the "BEST" software program.[16] The p$K_{a1}$, p$K_{a2}$, p$K_{a5}$, and p$K_{a6}$ values were assigned to the p$K_a$ values for the four amines in the cyclen ring by comparison with the p$K_a$ values for cyclen (L$^1$) and **5** (L$^5$),[10] as summarized in Table 1.

$$L \cdot H^+ \rightleftarrows L + H^+ \qquad K_a = [L]a_{H+}/[L \cdot H^+] \qquad (1)$$

The deprotonation behavior of **10** is shown in Scheme 5. Changes in the UV−vis absorption of **10** at 265 nm in the pH range 1−4 (Figure S1a in the Supporting Information), gave a sigmoidal curve (a) with closed squares in Figure 2a, which gave a p$K_a$ value of 2.7 ± 0.2, suggesting that the p$K_{a2}$ value of 2.5 determined by

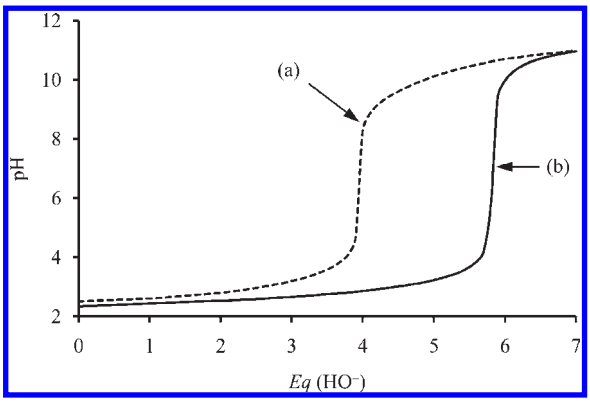


**Figure 1.** Typical potentiometric pH titration curves for (a) 1 mM $H_3L^6$ + 2 mM $HNO_3$ and (b) 1 mM $H_3L^6$ + 2 mM $HNO_3$ + 1 mM $Zn^{2+}$ with $I$ = 0.1 ($NaNO_3$) at 25 °C. *Eq* ($HO^-$) is the number of equivalents of base (NaOH) added.

**Table 1.** Deprotonation Constants ($pK_{ai}$) and Complexation Constants for Cyclen ($L^1$), **5** ($L^5$), and **10** ($L^6$) with $Zn^{2+}$ in Aqueous Solution with $I$ = 0.1 ($NaNO_3$) at 25 °C

| | cyclen ($L^1$) | **5** ($L^5$)[a] | **10** ($L^6$) |
|---|---|---|---|
| $pK_{a1}$ | < 2 | < 2 | < 2 |
| $pK_{a2}$ | < 2 | < 2 | < 2 |
| $pK_{a3}$ | 9.9 | < 2 | < 2 |
| $pK_{a4}$ | 11.0 | 7.2[b] | 2.51 ± 0.02[b]<br>2.7 ± 0.2[b,c] |
| $pK_{a5}$ | | 10.1 | 9.69 ± 0.02 |
| $pK_{a6}$ | | 11.5 | 10.84 ± 0.02 |
| log $K_s$(ZnL) | 16.2 | 22.4 | 19.5 |
| log $K_{app}$(ZnL) at pH 7.4 | 10.6 | 14.1 | 13.3 |
| log $K_{app}$(ZnL) at pH 5.0 | 5.5 | 10.8 | 9.0 |

[a] From ref 10. [b] The $pK_a$ values of 8-OH groups of quinolinol moieties. [c] The $pK_a$ value determined by pH-UV absorption profile.

potentiometric pH titration corresponds to the $pK_a$ value of the 8-OH group of **10** ($H_2L^6 \rightleftarrows H_2(H_{-1}L^6)$ in Scheme 5). Interestingly, this value is much smaller than those for **5** ($L^5$) (7.0) and **9b** (6.1) (See also Scheme 3).

Figure 3a shows an ORTEP drawing for the single-crystal X-ray structure of $H_2(H_{-1}L^6)$ (= $HL^6$), in which the 8-$O^-$ group of the quinolinolate moiety is hydrogen bonded to the ammonium cation of the cyclen ring. Representative crystallographic data for **10** ($HL^6$) and its $Zn^{2+}$ complex **11** ($Zn(H_{-1}L^6)$ displayed below are listed in Table 2. A space-filling model of the same crystal (Figure 3b) suggests that the 8-$O^-$ group of quinolinolate (O1 in Figure 3b) is surrounded by the quinoline ring, the $Me_2NSO_2$ group at the 7-position of 8-quinolinolate, and the cyclen ring. We, therefore, consider that the ion pair of Ar−$O^-$ (quinolinolate) and the ammonium group (cyclen ring) is stabilized in this hydrophobic space, resulting in the extremely lower $pK_a$ value of 2.5 in the ground state, compared to that for **9b** (6.1).[19]

**pH-Dependent Fluorescent Behaviors of 10 ($L^6$).** The pH-emission profile of **10** (excitation at 370 nm and emission at 478 nm) in Figure 2 (closed circles) shows a sigmoidal curve giving a $pK_a$ value of around 10−11 (See also Figure S1b in the Supporting Information). This $pK_a$ value obtained from emission spectra is much greater than the $pK_a$ value of 2.5−2.7 in the ground state determined by potentiometric pH and UV−vis titrations. For comparison, the emission intensity of **9b** is very small in the pH range of 2−13, as indicated by the open circles (c) in Figure 2. Therefore, this unique emission behavior of **10** can be attributed to the effect of its cyclen ring. Moreover, UV−vis absorption spectra of **10** at pH 10−12 showed negligible change, as displayed in Figure 2 and Figure S1 in the Supporting Information, supporting that the $pK_a$ value of around 10−11 obtained from pH−emission profile (Figure 2) corresponds to the $pK_a$ value of quinolinol group in **10** influenced by the cyclen ring in the excited state. We previously observed a similar phenomenon for **5** ($L^5$) and concluded that fluorescent quenching of quinolinols, which resulted in the higher $pK_a$ value obtained from emission spectra than that in the ground state, was due to the excited-state proton transfer (ESPT) from the cyclen ring.[20] Analogously, in the case of the anionic quinolinolate of the $H_2(H_{-1}L^6)$ (= $HL^6$) form or the $H(H_{-1}L^6)$ (= $L^6$) form, we assume that protons would be extracted from the protonated cyclen ring (its higher two $pK_a$ values, $pK_{a5}$ and $pK_{a6}$, are 9.7 and 10.8, respectively) in the exited states (Scheme 5), resulting in the quenching of its fluorescent emission.[21]

**UV−vis and Emission Titrations of 10 ($L^6$) with $Zn^{2+}$.** Figure 4a shows the results of the UV−vis absorption titration of 50 $\mu$M **10** ($L^6$) with $Zn^{2+}$ at pH 7.4 (10 mM HEPES with $I$ = 0.1 ($NaNO_3$)) and 25 °C. The absorption maximum shifted from 265 to 269 nm upon addition of the $Zn^{2+}$ (0−1.0 equiv) with isosbestic points at 284 and 370 nm.

As shown in Figure 4b, the emission of **10** (5 $\mu$M) was very weak at pH 7.4 and quantitatively increased with increasing $Zn^{2+}$ concentrations (excitation at 370 nm, which is an isosbestic point found in Figure 4a), reaching a plateau at 1.0 equiv with 32-fold increase in emission intensity at 478 nm (the inset of Figure 2b), which strongly indicated a 1:1 complexation of **10** with $Zn^{2+}$, considering together with the results of UV−vis titration.

Figure 5 shows a comparison of the pH-dependent changes in emission intensity of the two $Zn^{2+}$ complexes, **6** and **11** (5 $\mu$M). It is noteworthy that the fluorescent emission of **11** ($Zn(H_{-1}L^6)$, $\Phi_F$ = 0.41 at pH 7.4) is much greater than that of **6** ($Zn(H_{-1}L^5)$, $\Phi_F$ = 0.044 at pH 7.4), indicating that **10** is a more sensitive $Zn^{2+}$ probe than $L^5$. The facts that emission of **11** is almost constant at pH 4−11 and that the emission of **10** is very weak below pH 9

(19) As shown in Figure S2 in the Supporting Information, $H_2(H_{-1}L^6)$ was isolated as a dimeric structure. We cannot exclude the possibility that $\pi-\pi$ interactions between two quinolinol moieties from two separate molecules of $L^6$ could facilitate the deprotonation of the 8-OH groups.

(20) (a) Bardez, E.; Chatelain, A.; Larrey, B.; Valeur, B. *J. Phys. Chem.* **1994**, *98*, 2357–2366. (b) Bardez, E.; Devol, I.; Larrey, B.; Valeur, B. *J. Phys. Chem. B* **1997**, *101*, 7786–7793. (c) Cheatum, C. M.; Heckscher, M. M.; Crim, F. F. *Chem. Phys. Lett.* **2001**, *349*, 37–42. (d) Li, Q.-S.; Fang, W.-H. *Chem. Phys. Lett.* **2003**, *367*, 637–644.

(21) Prodi, Izatt, and Savage et al. reported that the fluorescent emission intensity of 7-methyl-8-quinolinol was much greater than that of 2-methyl-8-quinolinol, suggesting that a functional group at the 7-position affects the photochemical properties of 8-quinolinols. Bronson, R. T.; Montalti, M.; Prodi, L.; Zaccheroni, N.; Lamb, R. D.; Dalley, N. K.; Izatt, R. M.; Bradshaw, J. S.; Savage, P. B. *Tetrahedron* **2004**, *60*, 11139–11144.

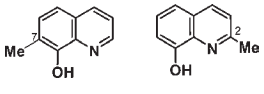

(Figures 2 and 4b) would permit a quantitative measurement of $Zn^{2+}$ to be made at pH 4−9.

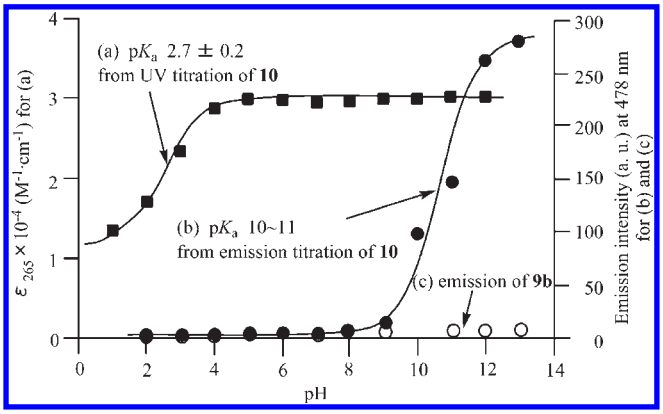


**Figure 2.** pH-dependent change in $\varepsilon_{265}$ (a) (closed squares) and emission intensity at 478 nm (b) (closed circles) for **10** ($L^6$) (excitation at 370 nm). [**10**] = 50 $\mu$M for UV−vis spectra and 5 $\mu$M for emission spectra in comparison with that of 5 $\mu$M **9b** at 478 nm (c, open circles).

**Complexation Behavior of 10 ($L^6$) with $Zn^{2+}$ As Studied by Potentiometric pH Titrations.** Analysis of a potentiometric pH titration curve for a mixture of 1 mM $H_3L^6$, 2 mM $HNO_3$, and 1 mM $ZnSO_4$ (curve b in Figure 1) with the "BEST" software program[16] gave a complexation constant defined by eq 2, log $K_s(Zn(H_{-1}L^6))$, of 19.5, from which the apparent complexation constants, log $K_{app}(Zn(H_{-1}L^6))$, were calculated to be 13.3 at pH 7.4 (dissociation constant, $K_d$, is 50 fM) and 9.0 at pH 5.0, respectively (See also Table 1). The $K_s(Zn(H_{-1}L^6))$ value for **11** is slightly smaller than that for **6**, possibly because of the electron-withdrawing effect of the $SO_2NMe_2$ at the 7-position. Figure 6 shows a distribution diagram for a mixture of 5 $\mu$M **10** ($L^6$) and 5 $\mu$M $Zn^{2+}$ obtained by calculation using the software program "SPE",[16] indicating that $Zn(H_{-1}L^6)$ is quantitatively formed at pH > 5 in micromolar concentrations.

$$K_s(Zn(H_{-1}L)) = [Zn(H_{-1}L)]/[H_{-1}L][Zn^{2+}] \quad (2)$$

$$K_{app}(Zn(H_{-1}L)) = [Zn(H_{-1}L)]/[L]_{free}[Zn^{2+}]_{free} \quad (3)$$

$$[L]_{free} = \sum [H_nL]_{free} \text{ at designated pH } (n = (-1)\sim 5) \quad (4)$$

**Scheme 5**

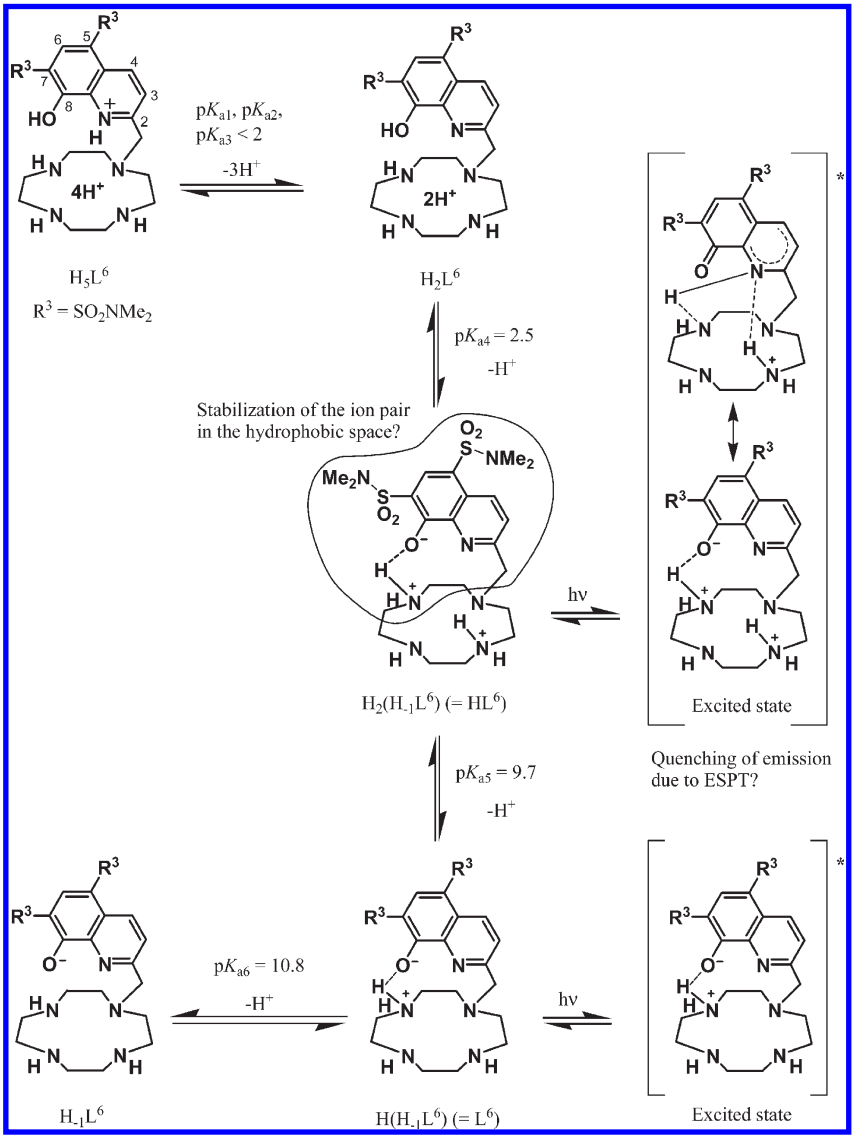

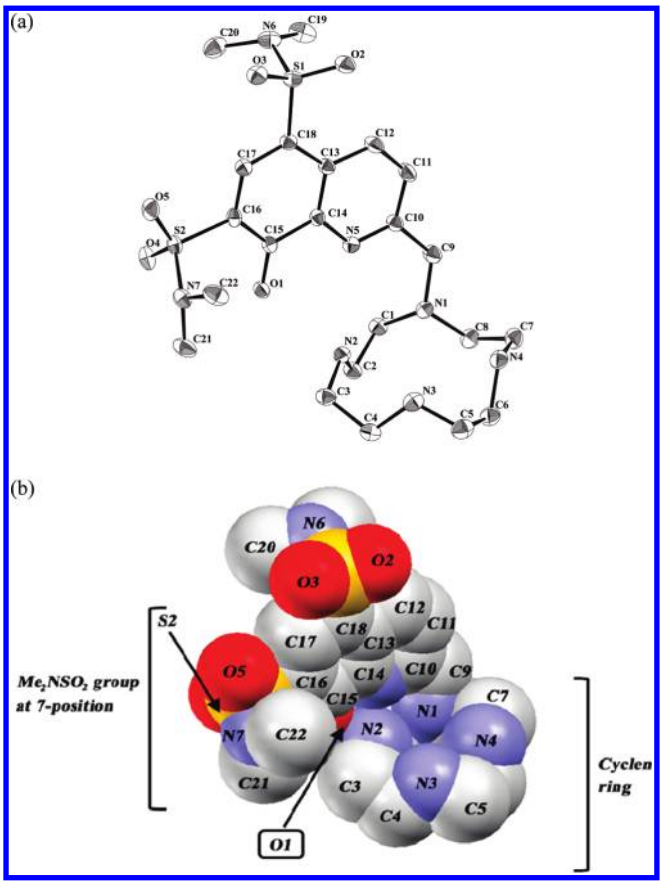


**Figure 3.** (a) ORTEP drawing (50% probability ellipsoids) of **10** $H_2(H_{-1}L^6)$ (= $HL^6$). Selected bond lengths [Å]: O(1)−C(15) 1.272(4), S(2)−C(16) 1.756(3), S(2)−N(7) 1.629(3), N(7)−C(22) 1.476(5), N(7)−C(21) 1.472(5). Water, hydrogen chloride and hydrogen atoms have been omitted for clarity. (b) Space-filling model of **10** $H_2(H_{-1}L^6)$ (= $HL^6$). The crystallographic parameters are given in Table 2.

**Table 2.** Crystallographic Data for **10** ($H_2(H_{-1}L^6)$ (= $HL^6$)) and **11** ($Zn(H_{-1}L^6)$)

| | **10**($H_2(H_{-1}L^6)$ (= $HL^6$)) | **11** ($Zn(H_{-1}L^6)$) |
|---|---|---|
| chemical formula | $C_{22}H_{50.4}Cl_1N_7O_{11.2}S_2$ | $C_{22}H_{36}N_8O_9S_2Zn_1$ |
| formula weight | 691.85 | 686.07 |
| space group | *C*2/*c* (#15) | $P2_1/n$ (#14) |
| *a* (Å) | 35.8779(7) | 11.602(5) |
| *b* (Å) | 19.7401(4) | 13.792(6) |
| *c* (Å) | 21.4880(7) | 17.941(8) |
| *β* (deg) | 118.8100(7) | 93.923(3) |
| *V* (Å$^3$) | 13334.9(6) | 2864(2) |
| *Z* | 16 | 4 |
| *T* (°C) | −180 | −140 |
| *λ* (Å) | 1.54187 | 0.71070 |
| $D_{calc}$ (g·cm$^{-3}$) | 1.378 | 1.591 |
| *μ* (Cu Kα for **10** and Mo Kα for **11**) (cm$^{-1}$) | 27.38 | 10.68 |
| *R1* ($I > 2\sigma(I)$) | 0.0685 | 0.0646 |
| *wR2* (all reflections) | 0.1966 | 0.1901 |

**X-ray Crystal Structure of 11 ($Zn(H_{-1}L^6)\cdot NO_3\cdot H_2O$).** Colorless crystals were obtained from a 1:1 mixture of **10** ($L^6$) and $Zn^{2+}$ in aqueous solution at pH 10. A single-crystal X-ray structure analysis disclosed that the $Zn^{2+}$ in **11** (Figure 7) is six-coodinated by the deprotonated O(1) at the 8-position of the quinoline ring, N(5) of the quinoline ring, and N(1)−N(4) of the cyclen ring, similar to the previously reported $Zn^{2+}$ complex **6**.[10] The bond lengths of Zn(1)−O(1), Zn(1)−N(1), Zn(1)−N(3), and Zn(1)−N(5) are 2.10−2.13 Å, which are shorter than Zn(1)−N(2) and Zn(1)−N(4). Four N atoms of the cyclen ring and the $Zn^{2+}$ ion form a tetragonal-pyramidal structure. Representative crystallographic parameters of **11** are listed in Table 2.

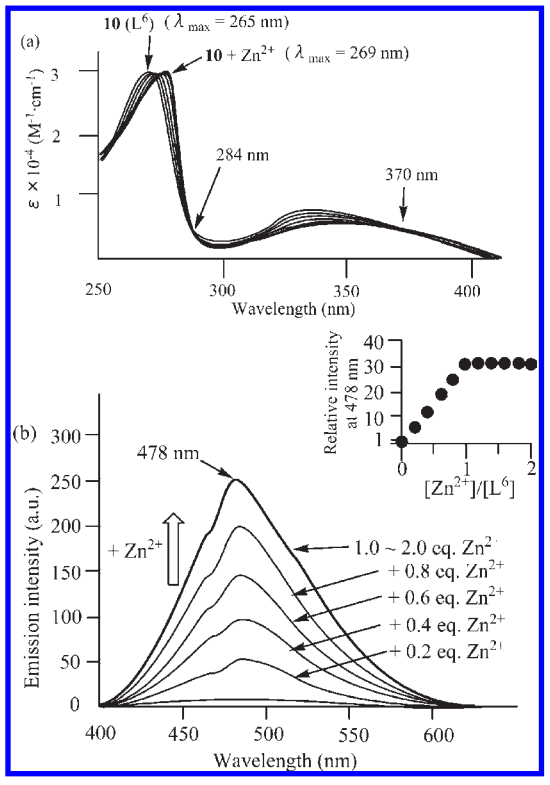


**Figure 4.** (a) Change in UV−vis spectra of 50 *μ*M **10** ($L^6$) with $Zn^{2+}$ (0−2.0 equiv), pH 7.4 (10 mM HEPES) with $I$ = 0.1 ($NaNO_3$) at 25 °C. (b) Change in the emission spectra of 5 *μ*M **10** ($L^6$) with $Zn^{2+}$ (0−2.0 equiv), pH 7.4 with $I$ = 0.1 ($NaNO_3$) at 25 °C (excitation at 370 nm). The inset shows the increase in the relative emission intensity of **10** ($L^6$) at 478 nm on the addition of $Zn^{2+}$.

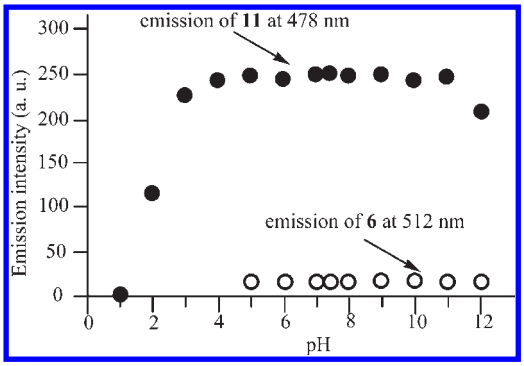


**Figure 5.** pH-Dependent change in the emission intensity of **6** ($Zn(H_{-1}L^5)$) (open circles) and **11** ($Zn(H_{-1}L^6)$) (closed circles) with $I$ = 0.1 ($NaNO_3$) at 25 °C (excitation at 338 nm for **6** and at 370 nm for **11**, [**6**] = [**11**] = 5 *μ*M). Arbitrary unit is a.u.

**Fluorescent Response of 10 to Various Metal Ions.** We examined the fluorescent response of **10** (5 *μ*M) to various metal ions in aqueous solutions at pH 7.4. As shown in Figure 8, **10** shows selectivity of fluorescent response to $Zn^{2+}$ (32 times emission enhancement) and $Cd^{2+}$ (41 times enhancement). When $Cu^{2+}$, $Co^{2+}$, $Mn^{2+}$, or $Fe^{2+}$ were added to **10** prior to the addition of $Zn^{2+}$, the increase in emission was inhibited. The results of UV−vis

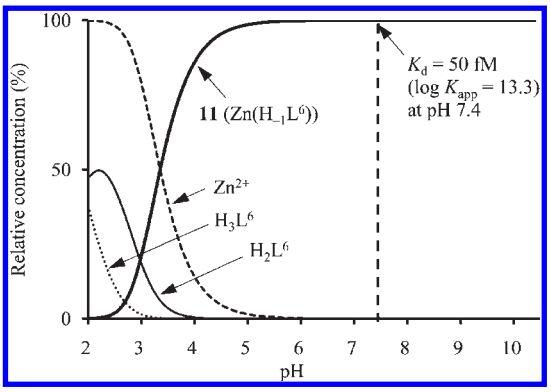


**Figure 6.** Distribution diagram for a mixture of 5 $\mu$M **10** ($L^6$) + 5 $\mu$M $Zn^{2+}$ with $I$ = 0.1 ($NaNO_3$) at 25 °C.

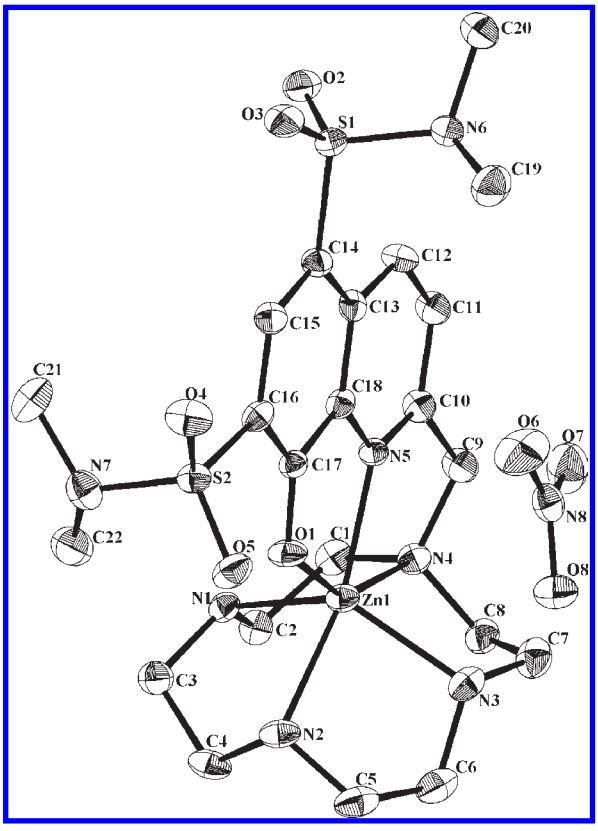


**Figure 7.** ORTEP drawing (50% probability ellipsoids) of **11** (Zn(H$_{-1}$L$^6$)). Selected bond lengths [Å]: Zn(1)−O(1) 2.123(2), Zn(1)−N(1) 2.129(3), Zn(1)−N(2) 2.229(3), Zn(1)−N(3) 2.126(3), Zn(1)−N(4) 2.427, Zn(1)−N(5) 2.103(3). Water and hydrogen atoms have been omitted for clarity.

titrations of **10** with $Cu^{2+}$, $Mn^{2+}$, $Co^{2+}$, and $Fe^{2+}$ suggested that **10** forms 1:1 complexes with these metal cations as shown in Figure S3 and S4 in the Supporting Information (the log $K_{app}$ values were estimated to be $> 10^8$ for $Cu^{2+}$, $Co^{2+}$, and $Mn^{2+}$, and $> 10^6$ for $Fe^{2+}$).[22] Therefore, the inhibition of the emission by these metal cataions could be attributed to competitive binding with $Zn^{2+}$ for **10** and/or quenching of the emission by paramagnetic metal cations.[23]

(22) The apparent complexation of **10** with $Fe^{2+}$ may be underestimated because of the UV−vis absorption of $Fe^{2+}$ itself at 250−600 nm.

(23) Lu, C.; Xu, Z.; Cui, J.; Zhang, R.; Qian, X. *J. Org. Chem.* **2007**, *72*, 3554–3557.

**$Zn^{2+}$-Dependent Hydrolytic Uncaging of 12.** As described in the Introduction, we reported on the synthesis of a benzenesulfonyl-caged (BS-caged) derivative of $L^5$ (**7**) in our previous report.[11] We then synthesized **12** in this study (Scheme 3) and tested $Zn^{2+}$-promoted hydrolytic uncaging, as evidenced by changes in UV−vis absorption spectra (Figure 9). While **12** was resistant to hydrolysis in the absence of $Zn^{2+}$ at pH 7.4, the addition of $Zn^{2+}$ triggered the increase in UV absorption at 269 nm with isosbestic points at 249, 281, and 329 nm, strongly suggesting the hydrolytic removal of the benzenesulfonyl moiety of **12** by Zn-bound $HO^-$ to give **11** (Zn(H$_{-1}$L$^6$)), as shown in Scheme 3. The $Zn^{2+}$-dependent hydrolysis of **12** was also confirmed by $^1$H NMR and UV−vis spectra measurements (Figures S5 and S6 in the Supporting Information).

Supporting Information, Figure S7 shows the time course for the hydrolysis of **12** at pH 5−9, from which the linear rate constants, $k_1$ ($sec^{-1}$), at pH 5.0, 6.0, 7.0, 7.4, 8.0, and 9.0 were determined and plotted in Figure 10a. The $k_1$-pH profiles for **12** gave a kinetic p$K_a$ value of 7.7 ± 0.2, which is in good agreement with the kinetic p$K_a$ values of 7.7 for **7**,[11] suggesting that the hydrolysis of **12** is promoted by Zn-bound $HO^-$. The data shown in figure 10a also indicates that the hydrolysis rate of **12** was much greater than that of **7** because of the electron-withdrawing effect of the $SO_2NMe_2$ group at the 7-position.

From an Eyring plot (the $1/T-\ln(k/T)$ profile in Figure 10b) for the hydrolytic uncaging of **12** (BS-caged-$L^6$) promoted by $Zn^{2+}$ or $Cd^{2+}$-bound $HO^-$, the Gibbs activation energy, $\Delta G^{\ddagger}$, the enthalpy of activation, $\Delta H^{\ddagger}$, and the entropy of activation, $\Delta S^{\ddagger}$, were calculated and the results were summarized in Table 3. The ($-T\Delta S^{\ddagger}$) values for the hydrolysis of **12** with $Zn^{2+}$ and $Cd^{2+}$ are nearly zero. We presume that hydrophobic and steric effect of the $Me_2NSO_2$ group at the 7-position of the quinoline moiety fix the conformation of the $PhSO_2$ group and hence restrict the transition states of the $Zn^{2+}$ and $Cd^{2+}$-promoted hydrolysis, resulting in negligible change in the degree of freedom (**18a** and **18b** in Scheme 6). The smaller $\Delta H^{\ddagger}$ value for the $Cd^{2+}$-promoted hydrolysis of **12** than that for the $Zn^{2+}$-promoted hydrolysis indicates the possibility of a different mechanism operating in these two reactions. The $Cd^{2+}$ ion, which has a larger ionic radius than that of $Zn^{2+}$, might be coordinated by the $PhSO_2$ moiety, resulting in a higher reactivity of the $PhSO_2$ group in **18** (Scheme 6).

**Measurement of $Zn^{2+}$ Concentrations in Sample Solutions by 12 (BS-caged-$L^6$).** We attempted to quantitatively measure [$Zn^{2+}$] in some sample solutions utilizing **12**. Essentially no change in the emission of **12** was observed in the absence of $Zn^{2+}$, as mentioned above, and the addition of given amounts of $Zn^{2+}$ (0−5 $\mu$M) followed by incubation at 25 °C for 30 min induced a nearly linear increase in emission, as shown in Figure S8 in the Supporting Information and Figure 11. In addition, it was found that this hydrolysis reaction of **12** with $Zn^{2+}$ completes within 10 min at 50 °C (Figure S6 in the Supporting Information), indicating that **12** has considerable potential for use in the quantitative analysis of $Zn^{2+}$ in solutions.

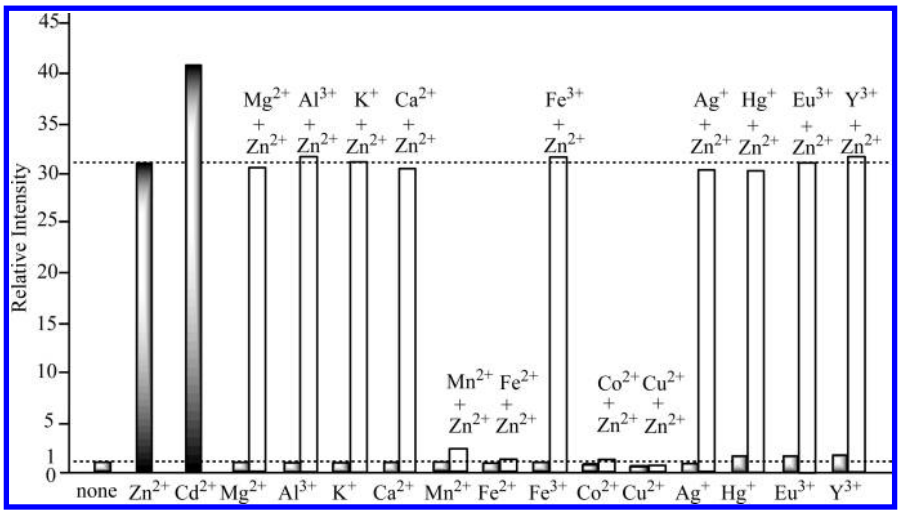


**Figure 8.** Fluorescent response of 5 $\mu$M **10** ($L^6$) at 478 nm to 1.0 equiv of various metal cations (shaded bars) and to 1.0 equiv of $Zn^{2+}$ added after 1.0 equiv of various metals (open bars) at pH 7.4 (10 mM HEPES) with $I$ = 0.1 ($NaNO_3$) at 25 °C.

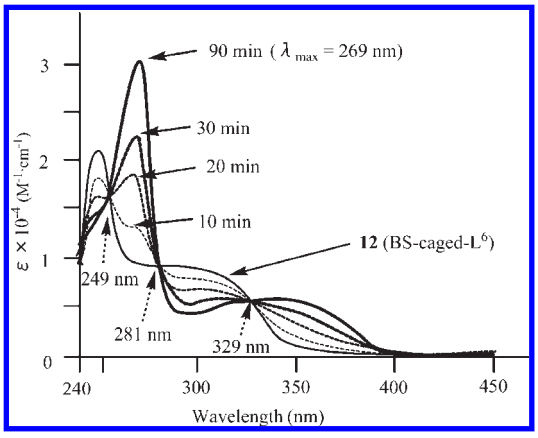


**Figure 9.** Change in UV−vis spectra as the result of the $Zn^{2+}$-promoted hydrolysis of 50 $\mu$M **12** (BS-caged-$L^6$) in the presence of 50 $\mu$M $Zn^{2+}$ at pH 7.4 (10 mM HEPES) with $I$ = 0.1 ($NaNO_3$) at 37 °C.

**Metal Selectivity in the Hydrolytic Uncaging of 12 (BS-caged-$L^6$).** We examined the hydrolytic uncaging of **12** (50 $\mu$M) in the presence of $Cd^{2+}$, $Cu^{2+}$, $Mn^{2+}$, $Co^{2+}$, $Fe^{2+}$, $Fe^{3+}$, $Ca^{2+}$, and $Mg^{2+}$ (50 $\mu$M each) at pH 7.4 at 25 °C, as evidenced by changes in UV−vis absorption spectra like Figure 9. We previously reported that the $Cd^{2+}$-catalyzed hydrolysis of **7** proceeds at almost same speed as $Zn^{2+}$-catalyzed hydrolysis.[11] Concerning **12**, hydrolysis by $Cd^{2+}$ was faster than that by $Zn^{2+}$. The $\varepsilon_{269}$ values increased in the presence of $Cu^{2+}$, $Mn^{2+}$, $Co^{2+}$, and $Fe^{2+}$, indicating that these metals promoted a partial hydrolysis of **12** (data not shown). The $\varepsilon_{269}$ value decreased with $Fe^{3+}$, possibly because of the complexation of **12** with $Fe^{3+}$ without hydrolysis.

**Photochemical Uncaging of 12 (BS-caged-$L^6$).** In our previous paper,[11] we reported that the benzenesulfonyl moiety of **7** can be removed by photoirradiation in aqueous solution to give **5** and benzenesulfonate (Scheme 2). Thus, we examined the photoreaction of **12**, as followed by UV−vis (Figure 12) and $^1$H NMR (Figure S9 in the Supporting Information) spectra. The UV−vis absorption curve for **12** (50 $\mu$M, curve (a) in Figure 12) changed to curve (b) after photoirradiation at 330 nm for 10 min in the absence of $Zn^{2+}$. Photoirradiation for 30 min gave curve (c), which agreed well with that of **10** (not shown). The fact that curves (a), (b), and (c) have an isosbestic point at 322 nm suggests that photolysis of **12** affords two main products **10** ($L^6$) and benzenesulfonate ($PhSO_3^-$), as proven by $^1$H NMR experiments (described below). Another isosbestic point at about 280 nm is not so clear, possibly because of the formation of $PhSO_3^-$ that

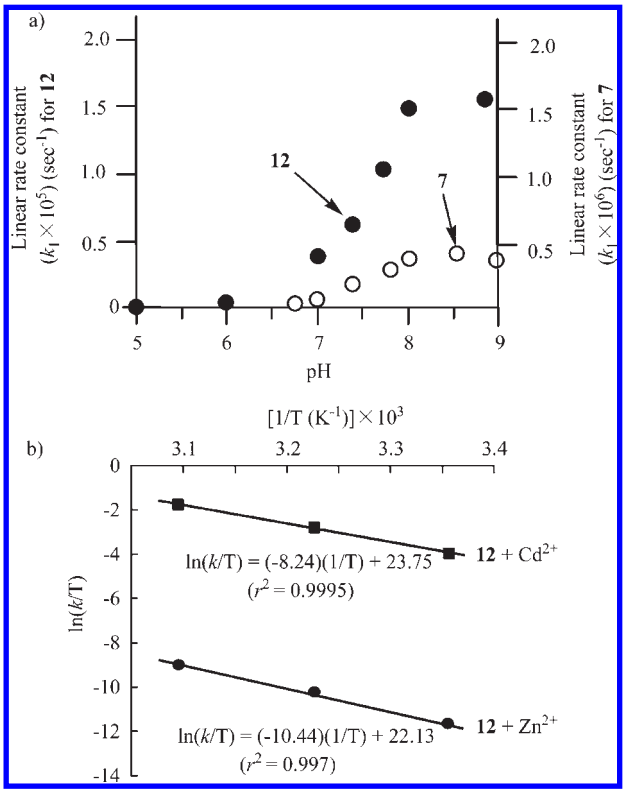


**Figure 10.** (a) pH-dependent plot of linear rate constants for the hydrolytic uncaging of **7** (BS-caged-$L^5$) and **12** (BS-caged-$L^6$) in the presence of $Zn^{2+}$ at 25 °C. (b) $1/T$−ln($k/T$) profile for the hydrolytic uncaging of **12** (BS-caged-$L^6$) promoted by $Zn^{2+}$ or $Cd^{2+}$-bound $HO^-$ ([**12**] = [$Zn^{2+}$] = [$Cd^{2+}$] = 50 $\mu$M in 10 mM HEPES (pH 7.4) with $I$ = 0.1 ($NaNO_3$)).

**Scheme 6**

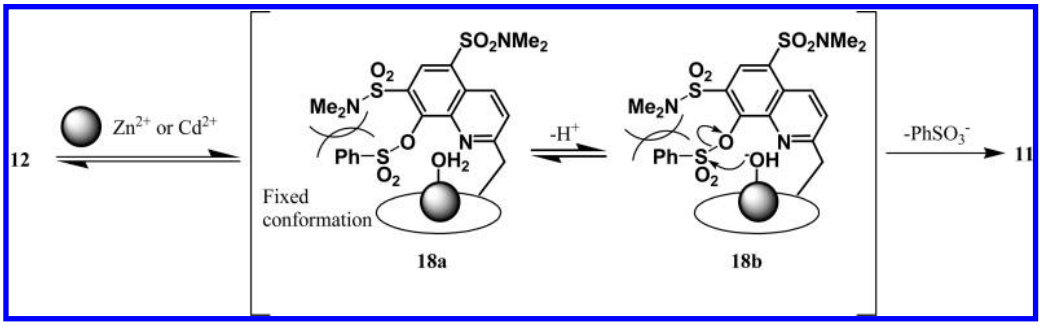


**Table 3.** Comparison of Activation Parameters for Hydrolysis of **7** and **12** Promoted by $Zn^{2+}$ or $Cd^{2+}$-bound $HO^-$ (pH 7.4 with $I$ = 0.1 ($NaNO_3$))[a]

| ligands | metals | $\Delta G^{\ddagger}$ (kcal/mol) | $\Delta H^{\ddagger}$ (kcal/mol) | $-T\Delta S^{\ddagger}$ (kcal/mol)[b] |
|---|---|---|---|---|
| **7** | $Zn^{2+}$ | 24[c] | 19[c] | 4.6[c] |
| **7** | $Cd^{2+}$ | 19[c] | 20[c] | −0.6[c] |
| **12** | $Zn^{2+}$ | 21 | 21 | 0.2 |
| **12** | $Cd^{2+}$ | 16 | 16 | 0.0 |

[a] [**7**] = [**12**] = [$Zn^{2+}$ or $Cd^{2+}$] = 50 $\mu$M. [b] $T$ = 298 K. [c] From ref 11.

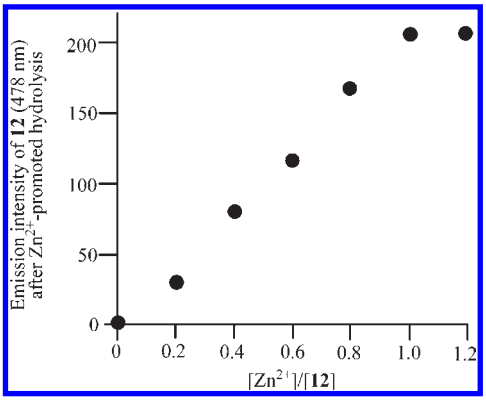


**Figure 11.** Quantitative increase in the fluorescent intensity of 5 $\mu$M **12** (BS-caged-$L^6$) by $Zn^{2+}$-dependent hydrolysis ([$Zn^{2+}$] = 0−6 $\mu$M) (emission was observed 478 nm with excitation at 370 nm) at pH 7.4 (10 mM HEPES with $I$ = 0.1 ($NaNO_3$)) and 37 °C (see also Figure S8 in the Supporting Information). Emission spectra were obtained by rapidly scanning the emission wavelength, to minimize photochemical uncaging (See below).

has small absorption at 240−290 nm ($\varepsilon_{260} \approx 0.6 \times 10^4$ $M^{-1}\cdot cm^{-1}$). The addition of 1.0 equiv of $Zn^{2+}$ to curve (c) gave curve (d) with an absorption maximum at 269 nm, strongly suggesting the formation of **10** ($Zn(H_{-1}L^6)$). The quantum yield for the photolysis of **12** (500 $\mu$M) was calculated to be $7.2 \times 10^{-5}$, which was greater than that of **7** ($2.3 \times 10^{-5}$).[11]

The photolysis of **12** (1 mM) in $D_2O$ at pD 7.4 was also confirmed by $^1H$ NMR experiments. After photoreactions for 30 and 90 min (irradiation at 330 nm), the spectra changed to those shown in Figures S9b and S9c in the Supporting Information, in which new $^1H$ signals appeared, showing good coincidence with those of **10** ($L^6$) (Figure S9d in the Supporting Information) and $PhSO_3^-$. Upon the addition of $Zn^{2+}$ to the solution shown in Figure S9c, Figure S9e was obtained, indicating the formation of **11** (Figure S9f). It is also noteworthy that the photolysis proceeded quantitatively with negligible byproducts being produced in aqueous solution. Our

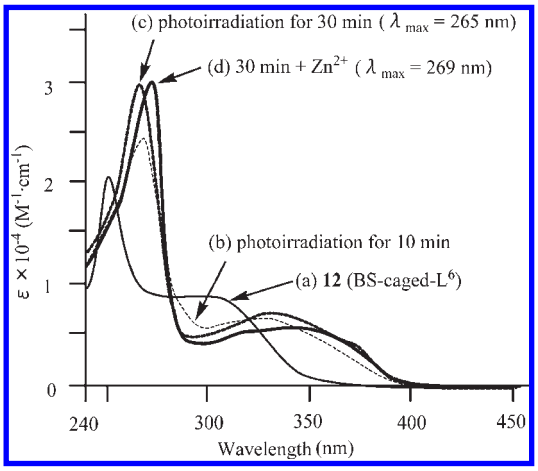


**Figure 12.** Photolysis of 50 $\mu$M **12** in pH 7.4 (10 mM HEPES with $I$ = 0.1 ($NaNO_3$)) at 25 °C (photoirradiation at 330 nm) followed by UV−vis absorption spectra. After 30 min of irradiation, 1.0 equiv of $Zn^{2+}$ was added into the reaction mixture.

recent study on the reaction mechanism involved in the photolysis of **7** (BS-caged-$L^5$), **12** (BS-caged-$L^6$), and some 8-quinolinyl sulfonate derivatives that have no cyclen unit suggested that this photolysis proceeds via homolytic S−O bond fission in the excited triplet state.[24]

**Comparison of Intracellular Concentrations of $Zn^{2+}$ Probes.** Intracellular concentrations of **2** ($L^2$), **5** ($L^5$), **10** ($L^6$), and **12** (BS-caged-$L^6$) in HeLa cells were estimated using our previously developed methods (concentrations of these probes: 50 $\mu$M, culture time: 0.5−1.0 h at 37 °C).[11] As summarized in Table 4, the intracellular concentration of **12** (10 ± 1 $\mu$M) was higher than **10** (2 ± 1 $\mu$M), possibly because of the presence of the two $Me_2NSO_2$ groups. Negligible cell damage was observed under these culture conditions.

**Fluorescent Staining of $Zn^{2+}$-loaded HeLa Cells.** Cell staining experiments of $Zn^{2+}$ in HeLa cells were performed using **10** and **12**. Figures 13a and 13b show phase contrast and fluorescent images of HeLa cells treated with 50 $\mu$M **10**. Figures 13c and 13d show data treated with 50 $\mu$M **10** for 0.5 h and then 25 $\mu$M $ZnSO_4$ and 20 $\mu$M $Zn^{2+}$ pyrithione ($Zn^{2+}$ carriers). Figures 13e and 13f show images of cells that had been treated with 50 $\mu$M **12** for 0.5 h and then 25 $\mu$M $ZnSO_4$ and 20 $\mu$M $Zn^{2+}$ pyrithione. These results indicate that **10** and **12** would be useful for detecting levels of intracellular $Zn^{2+}$.

(24) Kageyama, Y.; Oshima, R.; Sakurama, K.; Fujiwara, Y.; Tanimoto, Y.; Yamada, Y.; Aoki, S. *Chem. Pharm. Bull.* **2009**, *57*, 1257–1266.

**Table 4.** Estimated Intracellular Concentrations of $Zn^{2+}$ Fluorophores in HeLa Cells

| | **2** ($L^2$) | **5** ($L^5$) | **7** (BS-caged-$L^5$) | **10** ($L^6$) | **12** (BS-caged-$L^6$) |
|---|---|---|---|---|---|
| intracellular concentrations ($\mu$M) | $8 \pm 1^a$ | $0^a$ | $12 \pm 3^a$ | $2 \pm 1$ | $10 \pm 2$ |

[a] From ref 11.

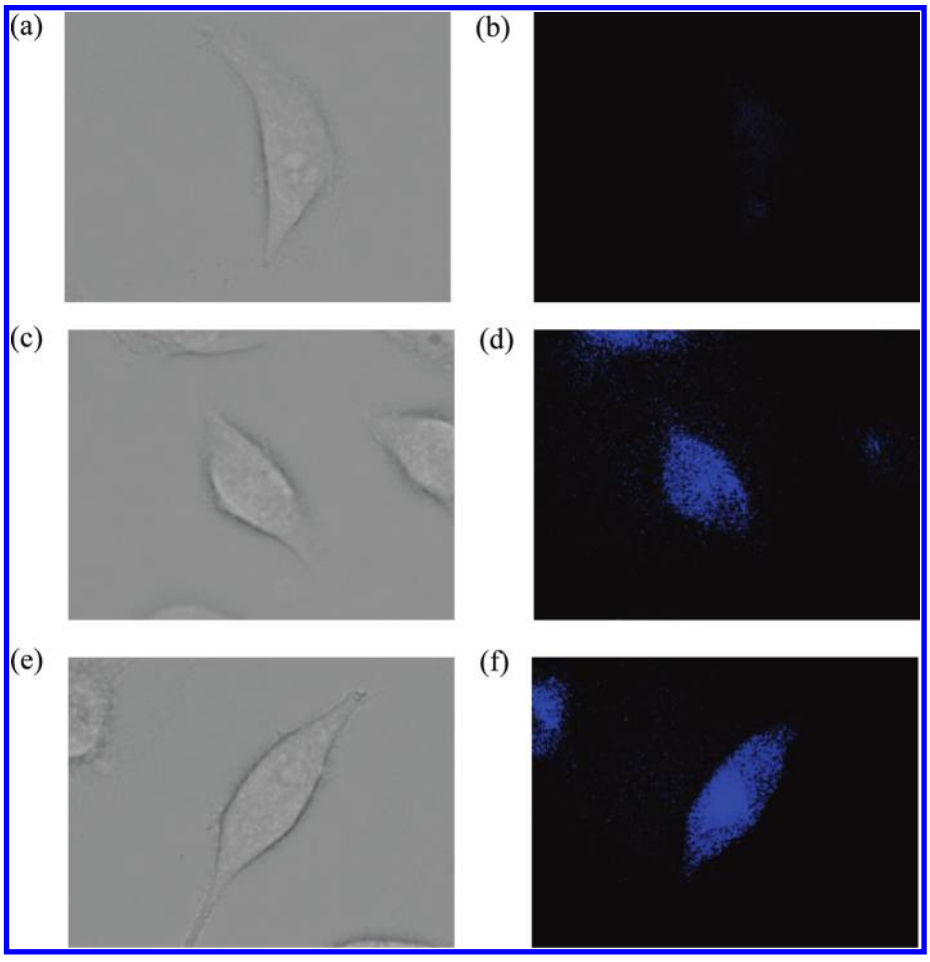


**Figure 13.** Microscopic images (×60 with digital zoom (×3.0)) of HeLa cells stained with 50 $\mu$M **10** without $Zn^{2+}$-pyrithione (a: phase contrast, b: fluorescent) and **10** (c: phase contrast, d: fluorescent) and **12** (e: phase contrast, f: fluorescent) with 25 $\mu$M $ZnSO_4$ and 20 $\mu$M pyrithione.

## Conclusion

A new $Zn^{2+}$ fluorophore **10** ($L^6$) was synthesized that has advantages over the previously described $Zn^{2+}$ probe **5** ($L^5$). The binding properties of **10** with $Zn^{2+}$ were comparable to that for **5**, while $Zn^{2+}$ sensitivity was improved considerably. We should note that the p$K_a$ value (p$K_a$ = ca. 10−11) of 8-OH group of quinolinol moiety of **10** in the exited state is much higher than the corresponding p$K_a$ value in the ground state (p$K_a$ = 2.5), which is much smaller than that of **9b** (p$K_a$ = 6.1) having no cyclen unit, permittng a quantitative measurement of $Zn^{2+}$ concentrations at neutral pH. A caged derivative of **12** (BS-caged-$L^6$) was also synthesized, and its uncaging properties were examined. The rapid uncaging of **12** by $Zn^{2+}$-dependent hydrolysis and $Zn^{2+}$-independent photolysis would be useful for $Zn^{2+}$ sensing. Even more efficient hydrolytic uncaging may be possible by introducing additional electron-withdrawing groups on the quinoline ring.[24] In addition, the staining of HeLa cells containing **10** and **12** was successful. Attempts to sense $Zn^{2+}$ in apoptotic cells are currently underway.

**Acknowledgment.** This work was supported by grants-in-aid from the Ministry of Education, Culture, Sports, Science and Technology (MEXT) of Japan (No. 18390009 and 19659026) and "Academic Frontier" project for private universities: matching fund subsidy from MEXT, 2009−2013. S.A. is grateful for grants from Mitsubishi Chemical Corporation Fund (Tokyo), the Terumo Life Pharmaceutical Research (Tokyo), the Novartis Foundation (Tokyo, Japan), the Naito Foundation (Tokyo), and the Tokuyama Science Foundation (Tokyo). M.K. is thankful for a grant-in-aid from MEXT of Japan (No. 20750081) and a Sasakawa Scientific Research Grant from the Japan Science Society.

**Supporting Information Available:** Figures S1−S9, tables, and CIFs for the X-ray crystal structure analysis of **10** ($H_2(H_{-1}L^6)$ (= $HL^6$)) and **11** ($Zn(H_{-1}L^6)$). This material is available free of charge via the Internet at http://pubs.acs.org.